



ISSN: 2350-0328

**International Journal of Advanced Research in Science,
Engineering and Technology**

Vol. 8, Issue 6 , June 2021

Modeling Of Linear Switched Reluctance Motor and Application

MOAMER MUSBAH MUHAMMED AHMED

Dept. of Electrical and Electronics Eng., University of Bani waleed

ABSTRACT: In this article, a switched reluctance linear motor is designed and investigated for use as a sliding door drive system. A two-dimensional nonlinear finite model is built to predict the performance of the engine being designed. Thus, the static electromagnetic characteristics are studied and analyzed. Inductance and electromagnetic force are determined for different transducer positions and current intensities taking into account the effects of magnetic saturation. The results of the analysis prove that the magnetic behavior of this motor is nonlinear. In addition, a significant asymmetry of the static and dynamic characteristics between the extreme phases and the central phase is observed at high excitation levels.

KEYWORDS: linear motor; sliding door; 2D-finite-element analysis; linear switched reluctance motor

I. INTRODUCTION

Recently, linear actuators are widely used in a large number of applications and are becoming increasingly used in many areas, particularly in industries such as transportation, manufacturing, and robotics [1-3]. Unlike conventional systems where linear motion is achieved by coupling a rotary actuator to a spherical screw system, a linear actuator allows for a direct linear actuator without the use of a rotary to linear transmission system. Then, it has fewer moving parts, so the inertia is low. In addition, linear actuators are recommended for applications that require high speed and precision [4], with this technology, the load is connected directly to the motor due to the lack of transmission systems, which translates into high performance capabilities and excellent dynamic characteristics. Because of these advantages and advantages, the linear actuator has been studied more and more in recent years [3], [5], [6], [7]. In reference [6], a ship crane vertical thrust actuator system with a linear switching frequency machine (LSRM) was designed and compared with conventional systems.

Electromechanical design requires accurate prediction of the developed forces. In fact, these forces are derived from field solutions obtained through numerical calculations. Several ways are used, but some seem to be able to achieve always accurate results. The advantages and disadvantages of each way were discussed in [8], [9]. Many ways have been reported in many businesses to predict the distribution of the magnetic field of electromagnetic structures, such as the method of obtaining network and analytical method [5-6] and limited-dimensional items [7] and 3D Items [8]. In this search, the methods of limited items have been used two-dimensional to study linear engine performance. The classic automatic opening device is usually with a rotary motor and transport systems. In such systems, the number of moving parts is great, which may increase the prospects of crashes and has negative effects on the dynamics and reliability of the system [10].

To improve performance and reduce the cost of sliding door systems, a linear actuator is introduced to supplement conventional systems. The first part of this article is dedicated to sizing linear frequency motors suitable for a sliding door application. In fact, the main dimensions and specifications of the engine are described. The second part is reserved for the modeling of the linear engine by the analytical method. This model can express the electromechanical conversion principles that govern the operation of a frequency-switched linear actuator, as an analytic relationship assuming the nonlinearity of the materials used. In the third part, a 2D finite element (FE) model is developed to study the electromagnetic properties, and a 2D FE model is used to analyze and study the static behavior of a linear actuator. The numerical solution of the developed model leads to the calculation of the magnetic vector voltage at each displacement step and the prediction of magnetic field density and magnetic force. The developed mechanical model was solved by the classical kinematic equation using a digital timer analyzer to obtain the dynamic properties. Then, the results obtained by analyzing the two-dimensional finite element method are presented. Finally, the fifth part describes the conclusion of the work.

II. SWITCHABLE LINEAR ACTUATOR SIZE

The device to be studied in this work for the application of sliding door is a three-phase linear planar structure (a, b, c). It consists of two magnetic parts, the stator is a toothed rod of equal distance and the translator is the moving part of the motor. The proposed motor has an active translator (with a coil), and consists of three units separated by a non-magnetic part, each unit representing a phase and containing two coils in series. The design of the linear actuator requires careful analysis of the required specifications, and the considered actuator provides a two-way force that moves a sliding door weighing 20 kg.

Figure 1 shows the structure and winding diagram of the designed motor.

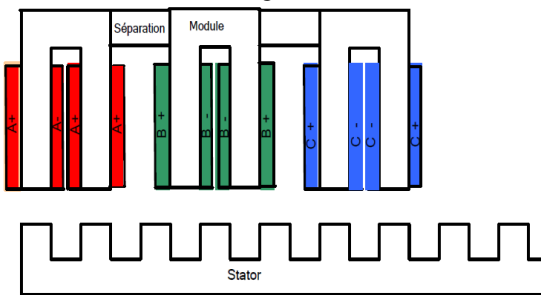


Fig. 1. Linear motor configuration and winding diagram

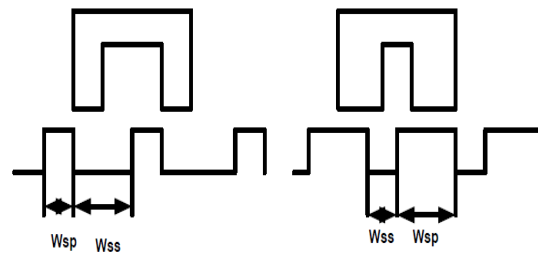


Fig. 2. Two elementary module configuration

The choice of the width of the motor teeth as well as the translator and stator must completely ensure reversibility and uniformity of movement. This is ensured by selecting an equal mileage between the translator and the stator. In addition, the width of the teeth and slots of the translator and stator should be equal, [5]. In fact, the inequality in tooth width and electrode inclination at the stator and moving units creates permeable steps around the equilibrium position, resulting in a dead zone on the static force properties that the rotor can move freely, Figure 2.

The pole width and slot width are related to the pole pitch by the following equation:

$$\lambda = w_{ts} + w_{tp} \tag{1}$$

Where w_{ts} is translator slot width, w_{tp} translator pole width.

The mover part includes three similar module shifted by a non magnetic separation has a width determinate by (2), [8].

$$c = c_o + k\lambda \tag{2}$$

The mechanical step δ_m is related to the pole pitch and the number of phases by (3).

$$\delta_m = |c_o - w_{ss}| = \frac{\lambda}{n} \tag{3}$$

The yoke thickness in the stator and in the translator is choosing equal to the slot width.

$$c_{sy} = c_{ty} = w_{ts} \tag{4}$$

The Fig.3 present a half crosses of the studied motor

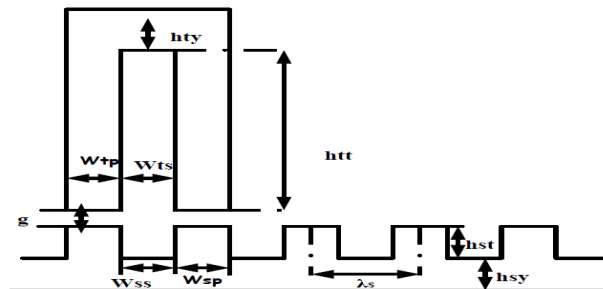


Fig. 3. Half Cross Section of the motor

The most significant geometry of the translator and stator are cited in the Table I:

TABLE I. SPECIFICATIONS OF DESIGNED MOTOR

	parameters	symbols	values
stator	Teeth width	W_{sp}	30mm
	Slots width	W_{ss}	30 mm
	Teeth high	H_{st}	30 mm
	Yocke thickness	C_{sy}	30 mm
translator	Teeth width	W_{tp}	30mm
	Slots width	W_{ts}	30mm
	Teeth high	H_{tt}	150mm
	Yocke thickness	C_{ty}	30mm
Coil	Number of turn	N	450
	Section of copper	S_c	$0.5mm^2$
separation	Width of separation	C	50mm
	Air gap	g	0.5mm

III. LINEAR MOTOR MODELING

The linear motor model is done in two stages, the first stage describes the electromagnetic equations, in the second stage the mechanical equations is developed.

A. Electromagnetic Equations

By neglecting the phase mutual effect, the phase voltage of the linear motor is related to the flux linked in the winding by Faraday's law as :

$$U = Ri + \frac{d\phi(x, i)}{dt} \quad (5)$$

Where i is the phase current, U is the terminal voltage , R is the phase winding resistance and Φ is the flux linkage.

The flux linkage in a linear motor phase varies as a function of the phase current and translator position, thus

$$U = Ri + \frac{\partial \phi}{\partial i} \cdot \frac{\partial i}{\partial t} + \frac{\partial \phi}{\partial x} \cdot \frac{\partial x}{\partial t} \quad (6)$$

The relation between flux and inductance is defined as follows:

$$\phi(x, i) = L(x, i)i \quad (7)$$

The characteristics of flux and inductance are determined by the 2D finite element method which will be presented subsequently. In general, the thrust force produced by the linear motors, derived from co energy.

When one phase is excited the electromagnetic force is written as follows:

$$F_x = \frac{\partial Wc(i, x)}{\partial x} \quad \text{Li} = cte \quad (8)$$

The coenergy of each phase can be calculated in terms of flux linkage.

$$Wc(i, x) = \int_0^i \phi(i, x) di \quad (9)$$

B. Mechanical Equation

The mechanical equation of the drive system is obtained by the Newton equation given by the following equation:

$$m \frac{d^2x}{dt^2} = f_x - f_c - f_0 \text{sign} \left(\frac{dx}{dt} \right) - \xi \frac{dx}{dt} \quad (10)$$

F_x : electromagnetic force (N)

$\frac{dx}{dt}$: linear speed ($\frac{m}{s}$)

m : moving part and load weight (Kg)

F_c : the load force (N)

F_0 : the dray coefficient

ζ : viscosity coefficient (N.s/m)

IV . 2-D FINAL ELEMENT ANALYSIS (FEA)

FEA is widely used to determine the performance of a designed machine and can provide an accurate prediction of characteristics. In this work, 2D FEA is used to predict the static and dynamic response of the motor under study.

A. Static characterization

The FE model was developed to study the static behavior of the proposed motor. In fact, the complete configuration of the FE model obtained using the engine specification is shown in Figure 4.

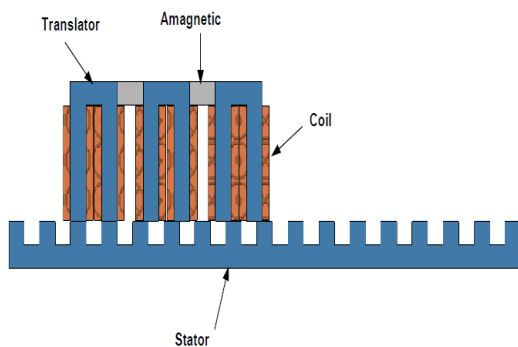


Fig. 4. Linear planner motor with modular configuration

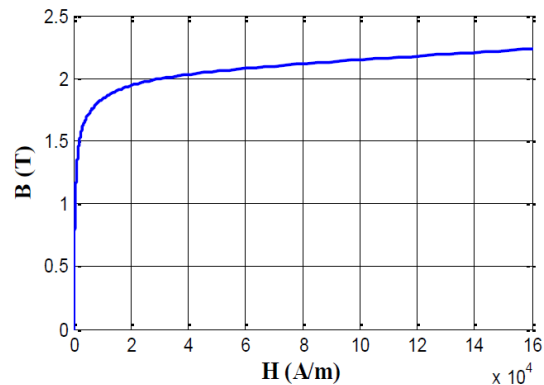


Fig. 5. The B-H curve of ferromagnetic material (1010 Steel)

The proposed structure of the three-phase motor, with the movable motor suspended on the fixed stator. The translator consists of three identical six-pole units with motor coils, and each unit has two poles and has the same pole pitch. The three units are spaced so that only two poles at a time can be aligned with the poles of the stator. Non-magnetic spacers are necessary between the different units in order to force a uniform displacement. The circuit coils are copper-plated and centered around the shaft of each unit, and the coils of the same phase are connected in series.

The material used to make the stator and translator is 1010 steel, and the magnetization curve corresponding to the latter material is shown in Figure 5. This curve has three distinct regions, the steep initial portion of the curve where a small increase in H leads to a large increase in B, the knee of the curve, and the saturated region behind the knee where a large increase in H includes a small increase in B. It can be seen from Figure 5 that A flux density of about 2 T indicates the onset of saturation in the material used.

The design of many electromechanical devices requires accurate prediction of the power developed. In fact, the designed structure of the proposed linear actuator is analyzed using a 2D nonlinear FEA, and then a series of simulations are run by a 2D static analyzer in order to calculate the binding values of electromagnetic force and flux for different translation positions during an electrical period. The calculated force obtained as a function of the positions of the translator is shown in Figs. 6 and Figure 7 for two phase excitation states 1200AT, 3000AT respectively.

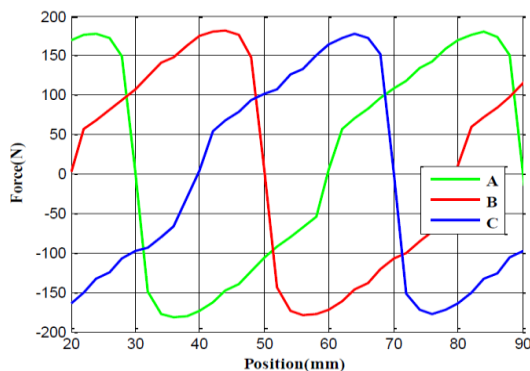


Fig. 6. Developed forces phases excited by 1200AT

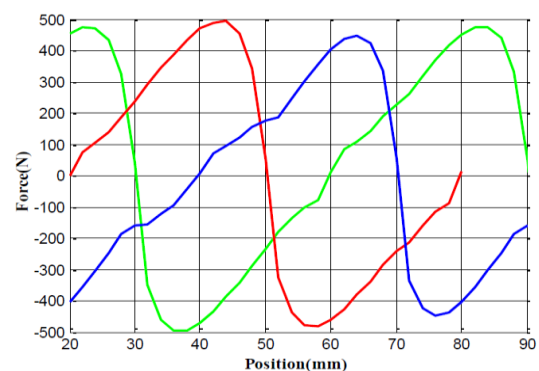


Fig. 7. Developed forces phases excited by 3000AT

The evolving forces shown in Fig. 6 and Fig. 7 indicate a large asymmetry between the extremes and the central phase. In the case of excitation current of about 3000Atrs, the maximum stage generates a maximum force of 500 N, while the central stage develops a maximum force of not more than 450 N. It is clear that the final effect occurs for high values of excitation d. The magnetic flux path and magnetic field density are shown in the figures below when the three phases A, B and C are excited respectively by 3000AT. The flux distribution in the actuator makes it possible to determine the degree of magnetic saturation in different parts of the device as well as the useful flux / leakage ratio through magnetic circuits.

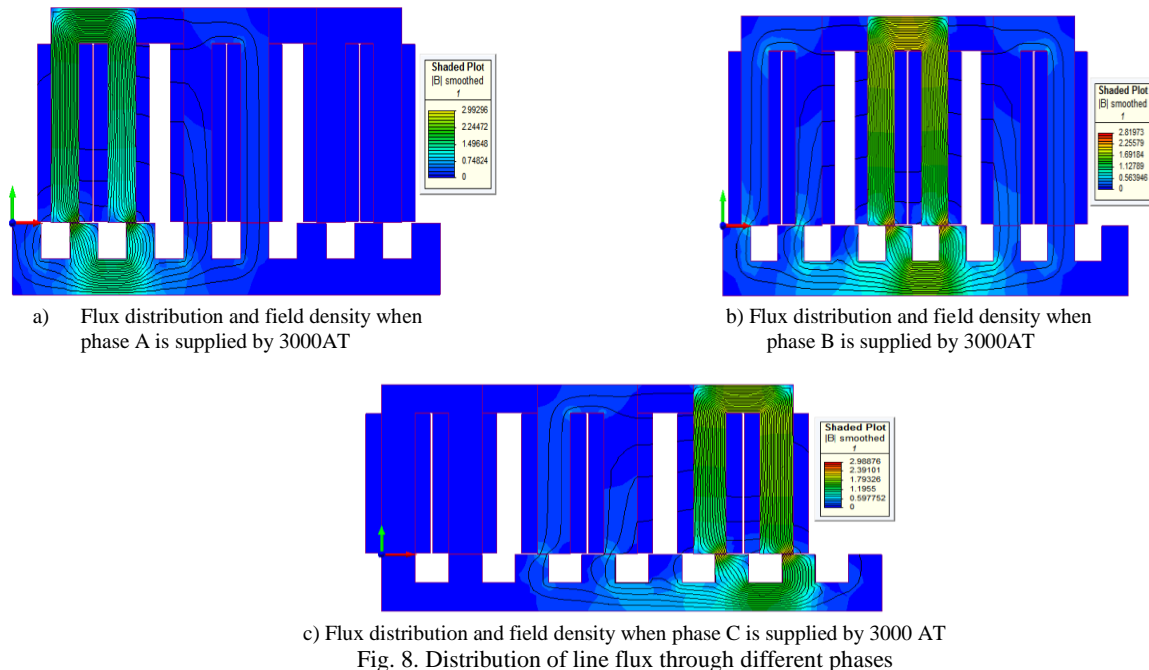


Fig. 8. Distribution of line flux through different phases

Analysis of the magnetic flux distribution for the same supplied current confirms that the magnetic asymmetry between the extreme phases and the phase at the center is due to magnetic leakage. The magnetic leakage in the central phase is greater than the extreme phases due to the flux flowing through adjacent units although there is a non-magnetic separator between them. Thus, these magnetic losses create parasitic forces that affect the performance of the machine. It is clear from Figure 8, that when the field current is 3000AT, magnetic saturation occurs at both ends of the pole of the stator and the translator. However, polar bodies are not saturated. The static characteristics of the linear machine are represented by the variation of the correlation of the flow with the amp-cycle phase and the location of the translator. Figure 9 shows the magnetization curve which is a plot of the flux association versus Ampersturn at three positions. These curves correspond, respectively, to the aligned, median, and unaligned position. The obtained flux curves as a function of ampere rotation are nonlinear and confirm the saturation of the material used for high values of excitation current.

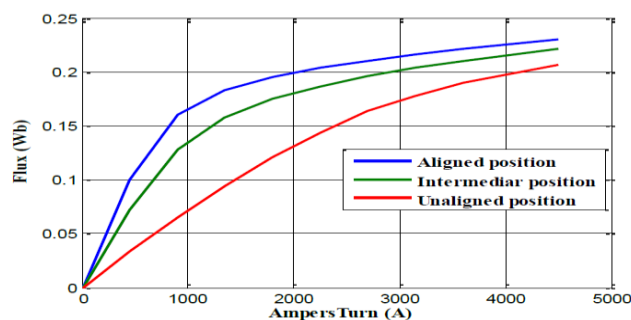


Fig. 9. Flux linkage as a function of ampere turn and translator position

In order to determine the profile of the inductance resorted the flux linkage equation given by (7). The graphic in figure 10 shows the curves of inductance with the translator position for different magneto-motive force values between 600Atrs to 3000Atrs, where the translator is moved from an aligned position to an unaligned position.

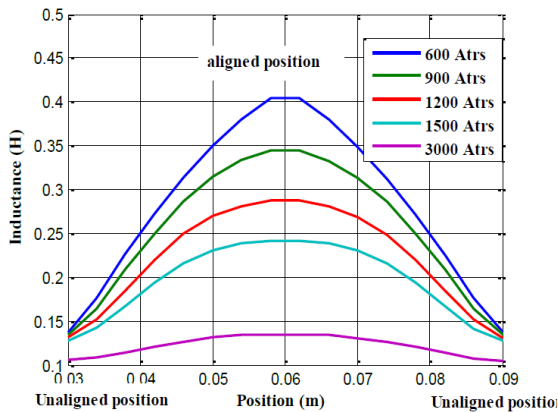


Fig. 10. Inductance-ampere turn characteristics

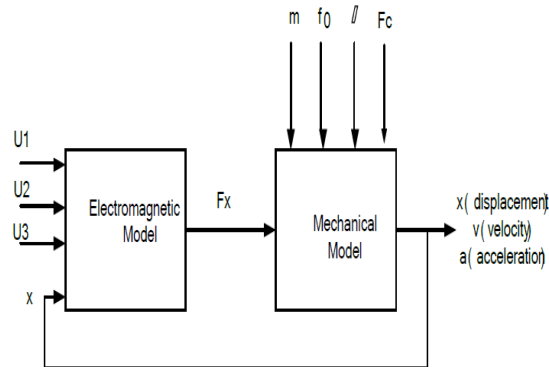


Fig. 11. Synopsis diagram

The obtained results show that the phase inductance in LSRM is a periodic function of the position of the translator, and the inductance curves are characterized by a maximum and a minimum value, these two values actually correspond to the aligned positions and are not aligned. The results show that at a given position of the translator, the phase inductance decreases with the applied phase current due to magnetic saturation. The phase induction in the aligned position varies greatly with the supplied current. However, the misaligned agitator did not change much, mainly due to the large reluctance that characterizes the large air gap in the flow path.

B. Dynamic response

The proposed linear actuator is designed for a direct drive system. Thus, it is important to study dynamic behavior. In this topic, a model by FE method is developed and used to predict the dynamic behavior of the proposed motor. In this work, a coupled electromagnetic-mechanical model is described for the transient analysis of a linear actuator, the mechanical parameters of the proposed structure are:

$$m = 20Kg, \xi = 65N \cdot \frac{s}{m}, f_0 = 0.1N$$

The simulation of the dynamic of the motor is done according to the synopsis schema bellow. In the following, we present the performances of the motor obtained by transient analysis FEM. The dynamic responses obtained are shown in Fig12-15.

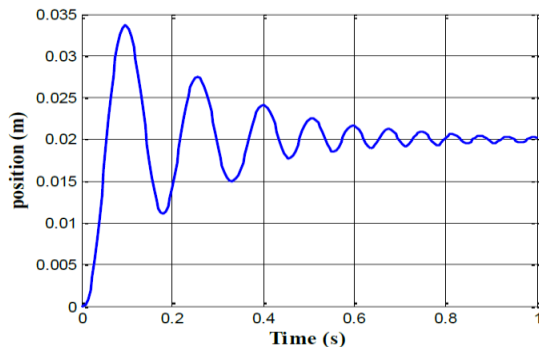


Fig. 12. Displacement versus time

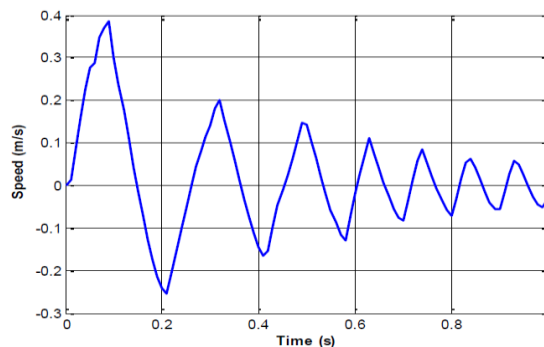


Fig. 13. Velocity versus time

The calculated displacement is obtained as a function of time when the coil is excited by 900Atrs, the moving part is initially offset by -20 mm from the aligned position, when only one phase is excited, the translator should move one step and stop at position (stable equilibrium position). The displacement characteristic shows oscillations about its equilibrium position equal to 20 mm corresponding to the initial displacement of the designed motor. In Figure 13, the rotor starts from zero velocity reaching a maximum of 0.38 m/s and then tilts towards zero at 1 s as the translator

reaches the rest position. It is clear from Figure 13 that the engine speed is characterized by strong oscillation and large overshoot.

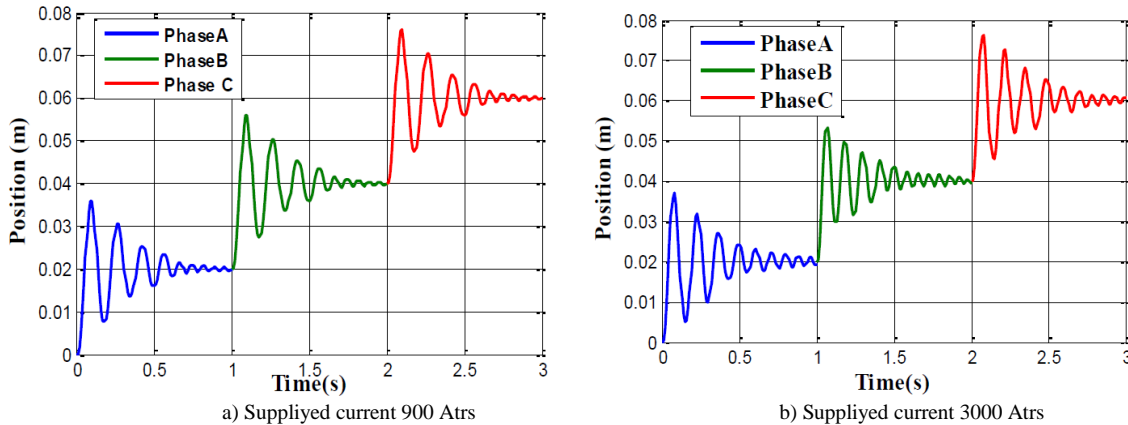


Fig. 14. Dynamic response of motor on three steps for two different currents

The displacement curve shown in Fig. 14 is obtained for two excitation current values corresponding to the linear region of the magnetization curve and the saturation region. The results obtained indicate that the process is in 3 consecutive mechanical phases without load when the single phase is excited for a fixed period.

The duration of each step is 1 second. Also, the presented result shows that at the first moment, stage A was excited to allow the translator to move to the first equilibrium position corresponding to 20 mm after B stage, and C should be excited respectively to obtain the other equilibrium position. Figure 14b shows that the overshoots and system response increase with increasing excitation current and display asymmetry between the external phases and central phase responses. Figure 15 shows the displacement characteristic when phase A is energized considering the effect of the load.

When a load force is applied to the system, the balance position of the linear actuator is affected by an error, and it appears that the displacement is accompanied by a large error with a high value of the load force. These phenomena affecting position accuracy can lead to loss of synchronization at high speed. To overcome such problems, a logical control method is required.

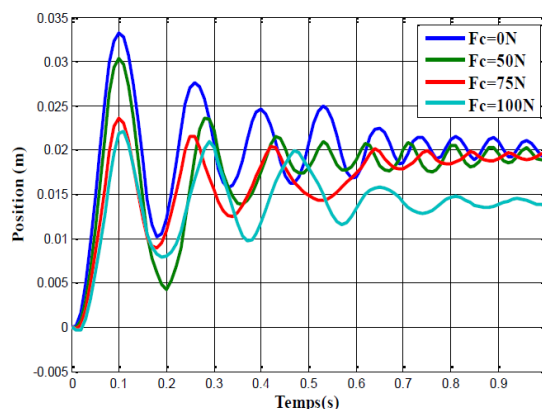


Fig. 15. Displacements versus time for different loads force

V. CONCLUSION

In order to improve the performance of traditional sliding door systems, a linear actuator has been proposed. In this paper, an approach to scaling and designing linear switching impedance is presented. For this reason, a finite element method was developed to calculate the static field and electromagnetic force generated by the chosen structure. In addition, a fundamental pattern FE analysis was performed using nonlinear magnetic materials considering saturation effects. The inductance and binding properties of the flow are presented and discussed depending on the position and current of the compiler.



ISSN: 2350-0328

International Journal of Advanced Research in Science, Engineering and Technology

Vol. 8, Issue 6 , June 2021

The obtained results showed a large asymmetry and magnetic leakage between the phases of the motor at high excitation levels. Based on the finite element method, dynamic properties such as displacement and velocity are obtained. Then, the effect of positional load was analyzed, and it was found that the difference of these parameters affects the positioning accuracy of the linear actuator.

In future research, an optimal control strategy should be developed to reduce the significant impact of the engine and improve its performance.

REFERENCES

- [1] N.S.Lobo, Hong Sun Lim R., Krishnan, "Comparison of linear switched reluctance machines for vertical propulsion application: Analysis, design, and experimental correlation," IEEE Transactions on industry applications, Vol.44, No.4, August 2008.
- [2] Lorand Szabo, Dan-Cristian Popa, Vasile Iancu "Compact double sided modular linear motor for narrow industria applications," Power Electronics and Motion, Conference IEEE, 2006.
- [3] F. Daldaban, N. Ustkoyuncu, "A novel linear switched reluctance motor for railway transportation systems," Energy Conversion and Management, 2010.
- [4] Lilia El Amraoui, "Conception électromagnétique d'une gamme d'actionneur Linéaire Tubulaire à Réductance variable," Thèse Doctorat en Génie Electrique, Ecole Centrale de Lille, 2002.
- [5] L. El Amraoui, F. Gillon, "Performance estimation of linear tubular actuator," Conferences maglev, 2002.
- [6] Hong Sun Lim, Hong Sun Lim, "Design and Control of a Linear Propulsion System for an Elevator Using Linear Switched Reluctance Motor Drives," IEEE transactions on industrial electronics, Vol. 55, No. 2, February 2008.
- [7] Abdulate.A.M.ELGANAI "The Corona Effect on High Voltage Transmission Lines". IJSETR International Journal of Scientific Engineering and Technology Research, ISSN 2319-8885 Volume.08, Jan-Dec-2019, Pages: 29-31
- [8] Abdulate.A.M.ELGANAI "Corona Losses Reliance from the Conductor Diameter Developed in Matlab/Simulink". IJSETR International Journal of Scientific Engineering and Technology Research, ISSN 2319-8885, Volume No.07, Issue No.12, December-2018, Pages: 1989-1993.
- [9] Mokrani Lakhdar, Contribution à la CAO optimisée des machines électriques, application au moteur linéaire à induction, thèse doctorat en Electrotechnique, Faculté des sciences de l'ingénieur de Batna, 2005.
- [10] M. Dursum, F. Koc, H. Ozbay, "Determination of geometric dimensions of a double sided linear switched reluctance motor," World Academy of Science Engineering and Technology, 46, 2010.
- [11] Zaafrane Wajdi, Khediri Jalel, Rehaoulia Habib, "Comparative design and modeling study of single sided linear planner switched reluctance motor," Wseas transactions on circuit and systems, volume 13, 2014.
- [12] J. G. Amoros, P. Andrada, "Sensitivity Analysis of Geometrical Parameters on a Double-Sided Linear Switched Reluctance Motor," IEEE Transactions on Industrial Electronics, VOL. 57, NO. 1, January 2010.
- [13] Khidiri Jalel, "Alimentation et commande d'un actionneur linéaire triphasé à flux transversale," Thèse de Docteur Ingénieur en Génie Electrique, Université des Science et Technique de Lille Flandres-Artois, 1986.
- [14] Zaafrane Wajdi, Khidiri Jalel, Rehaoulia Habib, "2-D finite element design of a single sided linear planner switched reluctance motor," World Applied Sciences Journal, 25 (3): 494-499, 2013.
- [15] Ge Baoming, Anibal T. de Almeida, "Design of Transverse Flux Linear Switched Reluctance Motor," IEEE transaction on magnetics, Vol. 45, No. 1, January 2009.
- [16] Ruiwu Cao, Ming Cheng, Chris Mi, "A linear doubly salient permanent magnet motor with modular and complementary structure," IEEE transaction on magnetics, Vol.47, No.12, December 2011.
- [17] S. Taghipour Boroujeni, J. Milimonfared, "Design prototyping and analysis of a novel tubular permanent magnet linear machine," IEEE transaction on magnetics, Vol.45, No.12, December 2009.
- [18] M. Jufer, "Traité d'électricité, électromécanique," traité d'électricité, électromécanique, Presses Polytechniques et Universitaires romandes, Lausanne 1995.
- [19] T.J.E. Miller, "Optimal design of switched reluctance Motors," IEEE Trans. Ind. Electron, Vol.49, no.1, pp.15-27, Feb. 2002.
- [20] R. Krishnan, R. Arumugam, and J.F. Lindsay, "Design procedure for switched reluctance motors," IEEE Trans. Ind. Appl, Vol.24, no.3, pp.456-461, May/Jun. 1988.
- [21] H.S. Lim and R. Krishnan, "Ropless elevator with linear switched reluctance motor drive actuation systems," IEEE Trans, Ind, Electron, Vol. 55, no.2, pp.534-542, Feb. 2008.
- [22] N.S. Lobo, H.S. Lim, and R. Krishnan, "Comparaison of linear switched reluctance machines for vertical propulsion application Analysis, design and experimental correlation," IEEE Trans. Appl, Vol.44, no.4, pp.1134-1142, Jul/Aug. 2008.
- [23] P.K. Budig, "The application of linear motors," In Proc. 3rd IEEE Int. Power Electron. and Motion Control Conf. Aug. 2000, vol.3, pp 1336-1341.